

Spectral method for the time-dependent Gross-Pitaevskii equation with a harmonic trap

Claude M. Dion and Eric Cancès

*CERMICS, École Nationale des Ponts et Chaussées,
6 & 8, avenue Blaise Pascal, Cité Descartes,
Champs-sur-Marne, 77455 Marne-la-Vallée, France*

(Dated: October 26, 2018)

Abstract

We study the numerical resolution of the time-dependent Gross-Pitaevskii equation, a non-linear Schrödinger equation used to simulate the dynamics of Bose-Einstein condensates. Considering condensates trapped in harmonic potentials, we present an efficient algorithm by making use of a spectral Galerkin method, using a basis set of harmonic oscillator functions, and the Gauss-Hermite quadrature. We apply this algorithm to the simulation of condensate breathing and scissors modes.

PACS numbers: 02.70.Hm, 03.75.Fi, 31.15.-p

I. INTRODUCTION

The experimental realization of Bose-Einstein condensation [1, 2, 3] has prompted much work on the study of the dynamics of these condensates. From the theoretical side, many interesting results have been obtained using the Gross-Pitaevskii equation (GPE) [4, 5, 6],

$$i\hbar\frac{\partial\Psi}{\partial t} = \left[-\frac{\hbar^2}{2m}\nabla^2 + V_{\text{ext}} + \frac{4\pi\hbar^2aN}{m}|\Psi|^2 \right] \Psi, \quad (1)$$

with the normalization condition $\|\Psi(t)\|_{L^2} = 1 \forall t$, to describe the order parameter Ψ (also called the *condensate wave function*) of N condensed bosons of mass m , interacting via a contact potential described by the scattering length a , and eventually confined by an external potential V_{ext} . Even though the Gross-Pitaevskii equation is based on the approximation that all bosons are in the condensed phase ($T = 0$ K), direct comparison between theoretical and experimental results have shown that, in many cases, solutions of the GPE contain the essential physics of the underlying phenomena [7, 8, 9, 10]. This non-linear Schrödinger equation (NLSE) has been used, in its time-dependent form, to investigate many aspects of the dynamics of Bose-condensed gas, such as the formation of vortices [11], the interference between condensates [12], of the possibility of creating atom lasers [13, 14], to mention only a few.

Most of these and other numerical studies of the time-dependent GPE are based on grid methods, i.e., discretize the spatial coordinates on a grid of points, the resulting differential equation being usually solved by Crank-Nicholson or split-operator Fourier methods (see, e.g., Refs. [15, 16, 17, 18]). We must point out that, while much care must be taken in solving Eq. (1) because of the non-linearity, we find, to our dismay, that many authors give results calculated with the time-dependent GPE without even specifying what method they have used for their numerical simulation.

In this article, we wish to focus our attention on the case where the Bose-Einstein condensate is in a (possibly anisotropic) harmonic trap, i.e.,

$$V_{\text{ext}}(X, Y, Z) = \frac{1}{2}m(\omega_x^2X^2 + \omega_y^2Y^2 + \omega_z^2Z^2) \quad (2)$$

which is the case for most experimental set-ups [19, 20]. The method we propose is based on the spectral decomposition of Ψ on a basis of harmonic-oscillator wave functions. In such a representation, the kinetic + trapping potential part of the Hamiltonian is diagonal. The

non-linear part is computed by forward and backward transformations from the spectral to a grid representation. By judicious use of the Gauss-Hermite quadrature, this can lead to an algorithm that is more efficient than those based on grid methods. Although this is akin to DVR methods based on Hermite polynomials, which have been successfully used for the time-independent and time-dependent GPE [21, 22], our method is distinct, since our Hamiltonian is expressed in the spectral representation for both the kinetic and potential operators.

We expose in Sec. II our spectral method and the resulting algorithm. We then present different time evolution schemes that can be used in combination with the spectral method. We finally give in Sec. IV some results that can be obtained from the numerical simulation of the time-dependent GPE, namely the study of condensate breathing and scissors modes.

II. SPACE DISCRETIZATION

To simplify the calculation, we will first rescale Eq. (1) in the three spatial dimensions (X, Y, Z) and in time,

$$X = \left(\frac{\hbar}{m\omega_x} \right)^{1/2} x \quad (3a)$$

$$Y = \left(\frac{\hbar}{m\omega_y} \right)^{1/2} y \quad (3b)$$

$$Z = \left(\frac{\hbar}{m\omega_z} \right)^{1/2} z \quad (3c)$$

$$t = \frac{1}{\omega_z} \tau. \quad (3d)$$

We also introduce a new wave function ψ defined as

$$\Psi(t, X, Y, Z) = A\psi(\tau, x, y, z)$$

and, considering the normalization condition

$$\int_{\mathbb{R}^3} |\Psi(t, X, Y, Z)|^2 dXdYdZ = 1 \quad \forall t,$$

we choose

$$A = \left(\frac{m}{\hbar} \right)^{3/4} (\omega_x \omega_y \omega_z)^{1/4}$$

such that

$$\int_{\mathbb{R}^3} |\psi(\tau, x, y, z)|^2 dx dy dz = 1.$$

The Gross-Pitaevskii equation therefore becomes

$$i \frac{\partial \psi}{\partial \tau} = \left[\frac{\omega_x}{\omega_z} \left(-\frac{1}{2} \nabla_x^2 + \frac{x^2}{2} \right) + \frac{\omega_y}{\omega_z} \left(-\frac{1}{2} \nabla_y^2 + \frac{y^2}{2} \right) + \left(-\frac{1}{2} \nabla_z^2 + \frac{z^2}{2} \right) + \lambda |\psi|^2 \right] \psi \quad (4)$$

with

$$\lambda = 4\pi a N \left(\frac{m \omega_x \omega_y}{\hbar \omega_z} \right)^{1/2}. \quad (5)$$

Coordinate z should be chosen such that ω_z is the greatest of the three frequencies [this is related to the arbitrary choice of the scaling factor in Eq. (3d)].

As all the physical parameters have been absorbed in the non-linear parameter λ , calculations with the same λ can correspond to results for different species, but in diverse experimental conditions. We can define acceptable lower and upper bounds for λ by considering the effective range of the different physical parameters. Considering only cases where the interparticle interaction is repulsive, i.e., $a > 0$ and therefore $\lambda > 0$, at the lower end we can consider a small $^4\text{He}^*$ condensate ($m = 4.0$ a.m.u., $a = 302$ a.u. [23]) of $N = 10^3$ atoms in a highly anisotropic $\omega_x \omega_y / \omega_z = 2\pi \times 10^{-1}$ Hz trap, giving $\lambda \approx 1.3$, while for a bigger $N \sim 10^6$ condensate of heavy atoms such as ^{87}Rb ($m = 86.9$ a.m.u., $a = 106$ a.u. [24]), λ can reach 10^5 for isotropic traps. In the following, we will restrict our study to λ in the range $1-10^3$, considering that the Thomas-Fermi approximation can be used for greater values of λ [21].

A. The spectral Galerkin method in 1D

For pedagogical purposes, we first explain our numerical method on the simple case of the one-dimensional NLSE

$$i \frac{\partial \psi}{\partial t}(t, x) = H_0 \psi(t, x) + \lambda |\psi(t, x)|^2 \psi(t, x) \quad (6)$$

with

$$H_0 = -\frac{1}{2} \frac{\partial^2}{\partial x^2} + \frac{1}{2} x^2.$$

Extensions to the three-dimensional case will be detailed in the next section.

Denoting by $\psi(t)$ the function $x \mapsto \psi(t, x)$, it can be proven [25] that if

$$\psi_0 \in \mathcal{X} := \left\{ \chi \in L^2(\mathbb{R}), \quad \int_{\mathbb{R}} \left| \frac{\partial \chi}{\partial x} \right|^2 < +\infty, \quad \int_{\mathbb{R}} x^2 |\chi(x)|^2 dx < +\infty \right\},$$

Eq. (6) with initial condition ψ_0 has a unique solution in $C^0([0, +\infty[, \mathcal{X}) \cap C^1([0, +\infty[, L^2(\mathbb{R}))$ and that both the L^2 norm

$$\|\psi(t)\|_{L^2} = \left[\int_{\mathbb{R}} |\psi(t, x)|^2 dx \right]^{1/2}$$

and the energy

$$E = (H_0 \psi(t), \psi(t)) + \frac{\lambda}{2} \int_{\mathbb{R}} |\psi(t, x)|^4 dx$$

are conserved by the dynamics. A variational formulation of Eq. (6), supplemented by the initial condition $\psi(t=0) = \psi_0$ where $\psi_0 \in \mathcal{X}$, reads

$$\begin{cases} \text{Search } \psi \in C^0([0, T], \mathcal{X}) \cap C^1([0, T], L^2(\mathbb{R})) \text{ such that} \\ \forall \chi \in \mathcal{X}, \quad i \frac{d}{dt}(\psi(t), \chi) = (H_0 \psi(t), \chi) + \lambda(|\psi(t)|^2 \psi(t), \chi) \\ \psi(0) = \psi_0. \end{cases} \quad (7)$$

Numerical solutions can then be obtained by approximating problem (7) with a Galerkin method: a *finite* dimensional subspace \mathcal{X}_N of the *infinite* dimensional vector space \mathcal{X} being given, we consider

$$\begin{cases} \text{Search } \psi_N \in C^1([0, T], \mathcal{X}_N) \text{ such that} \\ \forall \chi_N \in \mathcal{X}_N, \quad i \frac{d}{dt}(\psi_N(t), \chi_N) = (H_0 \psi_N(t), \chi_N) + \lambda(|\psi_N(t)|^2 \psi_N(t), \chi_N) \\ \psi_N(0) = \psi_0. \end{cases} \quad (8)$$

Denoting by (ϕ_0, \dots, ϕ_N) an orthonormal basis of X_N for the L^2 scalar product and by $C(t) = (c_n(t))_{0 \leq n \leq N}$ the vector of \mathbb{C}^{N+1} collecting the coefficients of $\psi_N(t)$ in the basis (ϕ_0, \dots, ϕ_N) , i.e.,

$$\psi_N(t, x) = \sum_{n=0}^N c_n(t) \phi_n(x),$$

problem (8) can be reformulated as

$$\begin{cases} \text{Search } C \in C^1([0, T], \mathbb{C}^{N+1}) \text{ such that} \\ i \frac{dC}{dt}(t) = hC(t) + \lambda F(C(t)) \\ C(0) = C_0 \end{cases} \quad (9)$$

where C_0 are the coefficients of ψ_0 and h the matrix of H_0 in the basis (ϕ_0, \dots, ϕ_N)

$$[C_0]_n = (\psi_0, \phi_n)_{L^2}, \quad h_{nm} = (H_0 \phi_m, \phi_n),$$

and where the function F is defined by

$$F(C)_n = \sum_{k,l,m=0}^N I_{klmn} c_k^* c_l c_m, \quad (10)$$

with

$$I_{klmn} = \int_{\mathbb{R}} \phi_k^* \phi_l \phi_m \phi_n^*.$$

The efficiency of a direct implementation [26, 27] of the Galerkin method described above is very poor: the calculation of the integrals I_{klmn} (which can be precomputed if the basis is small enough that the integrals can be stored in memory) scales as $O(N^4 N_p)$ where N_p is the number of grid points of the quadrature method, and the computation cost for one evaluation of the function F scales as N^4 [for each of the N coefficients, $O(N^3)$ operations are needed].

Our aim is to show that the Galerkin method becomes very efficient if (ϕ_0, \dots, ϕ_N) are the $N + 1$ lowest eigenmodes of the harmonic oscillator H_0 . In this case, indeed, the vector $F(C)$ can be computed *exactly* (up to round-off errors) in $O(N^2)$ operations. Let us recall that the eigenmodes $(\phi_n)_{n \in \mathbb{N}}$ of H_0 read

$$\phi_n(x) = \mathcal{H}_n(x) e^{-x^2/2},$$

where $\mathcal{H}_n(x)$ is the n -th Hermite polynomial [28], and that they satisfy

$$H_0 \phi_n = E_n \phi_n, \quad \text{with} \quad E_n = n + \frac{1}{2}.$$

In such a basis, the matrix h is therefore diagonal: $h = \text{Diag}(E_0, \dots, E_N)$. In addition, for any $C \in \mathbb{C}^{N+1}$, one has

$$F(C)_n = \int_{\mathbb{R}} |\psi(x)|^2 \psi(x) \phi_n(x) dx, \quad (11)$$

where $\psi(x) = \sum_{n=0}^N c_n \phi_n(x)$. The key point is now that for any $n \leq N$ the integrand in (11) is of the form $Q(x) e^{-2x^2}$, where $Q(x)$ is a polynomial of degree lower or equal to $4N$; each of the $N + 1$ integrals can therefore be computed *exactly* with a Gauss-Hermite quadrature formula involving $2N$ Gauss points [29]. More precisely, we have, for any polynomial Q of

degree lower or equal to $4N$,

$$\int_{-\infty}^{+\infty} Q(x)e^{-x^2} dx = \sum_{k=1}^{2N+1} w_k Q(x_k)$$

where $\{x_k\}$ are the roots of the Hermite polynomial \mathcal{H}_{2N+1} and where $\{w_k\}$ are convenient weights [30]. By a change of variable in integral (11), it follows that

$$F(C)_n = \sum_{k=1}^{2N+1} \left(\frac{w_k e^{x_k^2}}{\sqrt{2}} \right) \left| \psi \left(x_k / \sqrt{2} \right) \right|^2 \psi \left(x_k / \sqrt{2} \right) \phi_n \left(x_k / \sqrt{2} \right).$$

Spectral Galerkin methods are usually not very efficient [31]; but they can be in the specific case of the NLSE we are interested in because of the special form of the nonlinearity.

Let us now denote by $P \in \mathcal{M}(N+1, 2N+1)$ the matrix collecting the values of the basis functions $(\phi_n)_{0 \leq n \leq N}$ at the Gauss points $(x_k)_{1 \leq k \leq 2N+1}$:

$$P_{nk} = \phi_n \left(x_k / \sqrt{2} \right),$$

and by $\tilde{w}_k = w_k e^{x_k^2} / \sqrt{2}$. An efficient algorithm for the computation of $F(C)$ for a given $C \in \mathbb{C}^{N+1}$ reads:

1. Compute the vector $\Psi \in \mathbb{C}^{2N+1}$ defined by

$$\Psi = P^T \cdot C.$$

2. Compute the vector $\Xi \in \mathbb{C}^{2N+1}$ coefficient by coefficient along formula

$$\Xi_k = \tilde{w}_k |\Psi_k|^2 \Psi_k.$$

3. Compute

$$F(C) = P \cdot \Xi.$$

The vectors C and Ψ are the representation of the wave function ψ in the spectral basis $\{\phi_n\}_{0 \leq n \leq N}$ and in real space (at the $2N+1$ Gauss points $\{x_k / \sqrt{2}\}$), respectively. Steps 1 and 3 of the above algorithm scale quadratically in N (these are matrix-vector products), and step 2 scales linearly in N . We therefore end up with an algorithmic complexity in $O(N^2)$.

In practice, the function $C \mapsto F(C)$ is called one or several times at each time step; of course, the matrix P as well as the weights \tilde{w}_k can be precomputed once and for all and stored in memory.

B. The spectral-Galerkin method in 3D

Let us now turn to the 3D setting and consider the rescaled equation

$$i\frac{\partial\psi}{\partial t}(t, x, y, z) = \left[\frac{\omega_x}{\omega_z} H_0(x) + \frac{\omega_y}{\omega_z} H_0(y) + H_0(z) \right] \psi(t, x, y, z) + \lambda |\psi(t, x, y, z)|^2 \psi(t, x, y, z) \quad (12)$$

with

$$H_0(x) = -\frac{1}{2} \frac{\partial^2}{\partial x^2} + \frac{1}{2} x^2, \quad H_0(y) = -\frac{1}{2} \frac{\partial^2}{\partial y^2} + \frac{1}{2} y^2, \quad H_0(z) = -\frac{1}{2} \frac{\partial^2}{\partial z^2} + \frac{1}{2} z^2.$$

For $\lambda \geq 0$, a global-in-time existence and uniqueness result is available for Eq. (12) with initial condition $\psi(t=0) = \psi_0$ and

$$\psi_0 \in \mathcal{X} = \left\{ \chi \in L^2(\mathbb{R}^3), \quad \nabla \chi \in (L^2(\mathbb{R}^3))^3, \quad (x^2 + y^2 + z^2)^{1/2} \chi \in L^2(\mathbb{R}^3) \right\}.$$

On the other hand, it is well known that finite-time blow-up may be observed for $\lambda < 0$ and for some initial conditions [25]. As stated above, we focus here on the case where $\lambda \geq 0$.

Following the same lines as in the Sec. II A, the approximated wave function $\psi_N(t)$ is expanded on the spectral tensor basis set

$$(\phi_{n_x}(x) \phi_{n_y}(y) \phi_{n_z}(z))_{0 \leq n_x \leq N_x, 0 \leq n_y \leq N_y, 0 \leq n_z \leq N_z}.$$

One therefore has

$$\psi_N(t, x, y, z) = \sum_{n_x=0}^{N_x} \sum_{n_y=0}^{N_y} \sum_{n_z=0}^{N_z} c_{n_x n_y n_z}(t) \phi_{n_x}(x) \phi_{n_y}(y) \phi_{n_z}(z). \quad (13)$$

The equation satisfied by the three index tensor $C = [c_{n_x n_y n_z}]$ in the Galerkin approximation formally has the same expression as in 1D,

$$i\frac{dC}{dt}(t) = hC(t) + \lambda F(C(t)),$$

the linear operator h now being defined by

$$[hC]_{n_x n_y n_z} = E_{n_x n_y n_z} c_{n_x n_y n_z}$$

with

$$E_{n_x n_y n_z} = \frac{\omega_x}{\omega_z} \left(n_x + \frac{1}{2} \right) + \frac{\omega_y}{\omega_z} \left(n_y + \frac{1}{2} \right) + \left(n_z + \frac{1}{2} \right),$$

and the non-linear function $F(C)$ by

$$[F(C)]_{n_x n_y n_z} = \int_{\mathbb{R}^3} |\psi(x, y, z)|^2 \psi(x, y, z) \phi_{n_x}(x) \phi_{n_y}(y) \phi_{n_z}(z) dx dy dz,$$

where $\psi(x, y, z)$ is given by Eq. (13).

Let us denote by $\{x_k\}_{1 \leq k \leq 2N_x+1}$, $\{y_k\}_{1 \leq k \leq 2N_y+1}$, $\{z_k\}_{1 \leq k \leq 2N_z+1}$ the roots of the Hermite polynomials \mathcal{H}_{2N_x+1} , \mathcal{H}_{2N_y+1} , \mathcal{H}_{2N_z+1} and $\{w_k^x\}_{1 \leq k \leq 2N_x+1}$, $\{w_k^y\}_{1 \leq k \leq 2N_y+1}$, $\{w_k^z\}_{1 \leq k \leq 2N_z+1}$ the associated summation weights. Let us also introduce the matrices $P_x \in \mathcal{M}(N_x + 1, 2N_x + 1)$, $P_y \in \mathcal{M}(N_y + 1, 2N_y + 1)$, $P_z \in \mathcal{M}(N_z + 1, 2N_z + 1)$ defined by

$$[P_x]_{n_x k_x} = \phi_{n_x}(x_{k_x}/\sqrt{2}), \quad [P_y]_{n_y k_y} = \phi_{n_y}(y_{k_y}/\sqrt{2}), \quad [P_z]_{n_z k_z} = \phi_{n_z}(z_{k_z}/\sqrt{2}),$$

and the weights

$$\tilde{w}_{k_x}^x = \frac{w_{k_x}^x e^{x_{k_x}^2}}{\sqrt{2}}, \quad \tilde{w}_{k_y}^y = \frac{w_{k_y}^y e^{y_{k_y}^2}}{\sqrt{2}}, \quad \tilde{w}_{k_z}^z = \frac{w_{k_z}^z e^{z_{k_z}^2}}{\sqrt{2}}.$$

The following algorithm for the computation of $F(C)$ scales in $O(NN_xN_yN_z)$ where $N = \max(N_x, N_y, N_z)$:

1. Set $\Psi^{SSS} = C$
2. Compute $\Psi_{n_x n_y k_z}^{SSR} = \sum_{n_z=0}^{N_z} [P_z]_{n_z k_z} \Psi_{n_x n_y n_z}^{SSS}$ $O(N_x N_y N_z^2)$ operations
3. Compute $\Psi_{n_x k_y k_z}^{SRR} = \sum_{n_y=0}^{N_y} [P_y]_{n_y k_y} \Psi_{n_x n_y k_z}^{SSR}$ $O(N_x N_y^2 N_z)$ operations
4. Compute $\Psi_{k_x k_y k_z}^{RRR} = \sum_{n_x=0}^{N_x} [P_x]_{n_x k_x} \Psi_{n_x k_y k_z}^{SRR}$ $O(N_x^2 N_y N_z)$ operations
5. Compute $\Xi_{k_x k_y k_z}^{RRR} = \tilde{w}_{k_x}^x \tilde{w}_{k_y}^y \tilde{w}_{k_z}^z |\Psi_{k_x k_y k_z}^{RRR}|^2 \Psi_{k_x k_y k_z}^{RRR}$ $O(N_x N_y N_z)$ operations
6. Compute $\Xi_{k_x k_y n_z}^{RRS} = \sum_{k_z=1}^{2N_z+1} [P_z]_{n_z k_z} \Xi_{k_x k_y k_z}^{RRR}$ $O(N_x N_y N_z^2)$ operations
7. Compute $\Xi_{k_x n_y n_z}^{RSS} = \sum_{k_y=1}^{2N_y+1} [P_y]_{n_y k_y} \Xi_{k_x k_y n_z}^{RRS}$ $O(N_x N_y^2 N_z)$ operations
8. Compute $\Xi_{n_x n_y n_z}^{SSS} = \sum_{k_x=1}^{2N_x+1} [P_x]_{n_x k_x} \Xi_{k_x n_y n_z}^{RSS}$ $O(N_x^2 N_y N_z)$ operations
9. Set $F(C) = \Xi^{SSS}$.

In the above formulation, the superscripts S and R stand for *spectral* and *real space* representations respectively. In other words, steps 2–4 constitute the successive transform of the wave function from the spectral basis to a spatial representation on the series of points of

the Gauss-Hermite quadrature. The non-linear term of the Hamiltonian is then calculated in this spatial representation (step 5), while steps 6–8 correspond to the inverse transform back to the spectral basis. It is this procedure of forward and backward transformation that allows us to obtain a much better scaling than the implementation of Eq. (10).

The scaling of the above algorithm [$O(N^4)$ if $N_x = N_y = N_z$] has to be compared with the scaling of FFT based algorithms which scale in $O(N_p^3 \log(N_p))$ where N_p is the number of grid points per direction. The main interest of the spectral method is that for a similar accuracy, the number of spectral basis functions per direction (here denoted by N) can usually be chosen much smaller than the number N_p of grid points per direction. This is especially true when the problem considered displays a symmetry in one or more of the directions, in which case the basis set used in the Galerkin approximation Eq. (13) can be restricted to even harmonic oscillator functions (in the corresponding direction). We will come back on this important feature of the spectral method in Section IV.

C. Exploiting spherical or cylindrical symmetry

When $\omega_x = \omega_y = \omega_z$ the one-particle Hamiltonian possesses spherical symmetry. If the initial condition $\psi_0 = \psi(t = 0)$ has the same symmetry, then the wave function $\psi(t)$ is spherical symmetric for any $t > 0$: $\psi(t, x, y, z) = \psi(t, r)$ where $r = (x^2 + y^2 + z^2)^{1/2}$, is the radial coordinate. Eq. (4) leads to the effective 1D dynamics

$$i \frac{\partial \psi}{\partial t} = \left[-\frac{1}{2r^2} \frac{\partial}{\partial r} \left(r^2 \frac{\partial}{\partial r} \right) + \frac{r^2}{2} + \lambda |\psi|^2 \right] \psi. \quad (14)$$

Let us now define the function

$$\chi(t, r) = \begin{cases} \sqrt{2\pi} r \psi(t, r) & \text{if } r > 0 \\ -\sqrt{2\pi} r \psi(t, -r) & \text{if } r < 0. \end{cases}$$

It is easy to check that χ actually satisfies the 1D NLSE

$$i \frac{\partial \chi}{\partial t} = H_0 \chi + \lambda \frac{|\chi|^2}{2\pi r^2} \chi.$$

Besides, for any $t > 0$ the function $\chi(t) : r \mapsto \chi(t, r)$ is odd and belongs to $L^2(\mathbb{R})$ since

$$\int_{-\infty}^{+\infty} |\chi(t, r)|^2 dr = \int_0^{+\infty} 4\pi r^2 |\psi(t, r)|^2 dr = 1.$$

It can thus be expanded on the *odd* modes of the harmonic oscillator:

$$\chi(t, r) = \sum_{n=0}^{+\infty} c_n(t) \phi_{2n+1}(r).$$

A spectral Galerkin approximation can now be used. The vector $C(t) \in \mathbb{C}^{N+1}$ collecting the coefficients $(c_k(t))_{0 \leq k \leq N}$ of the approximated wave function

$$\chi_N(t, r) = \sum_{n=0}^N c_n(t) \phi_{2n+1}(r)$$

obeys once again a dynamics of the form

$$i \frac{dC}{dt}(t) = hC(t) + \lambda F(C(t)).$$

Here

$$h = \text{Diag}(E_{2n+1}), \quad \text{with} \quad E_{2n+1} = 2n + \frac{3}{2},$$

and

$$[F(C)]_n = \int_{\mathbb{R}} \frac{|\chi(r)|^2}{2\pi r^2} \chi(r) \phi_{2n+1}(r) dr,$$

where $\chi(r) = \sum_{n=0}^N c_n \phi_{2n+1}(r)$. As for any $0 \leq n \leq N$, $\phi_{2n+1}(r) = r P_{2n}(r) e^{-r^2/2}$ where P_{2n} is a polynomial of degree equal to $2n$, it follows that the above integrals can be computed exactly with $4N$ Gauss points.

Let us now turn to the cylindrical symmetry when (for instance) $\omega_x = \omega_y$ and when the initial data reads $\psi_0(x, y, z) = \psi_0(r, z)$ with $r = (x^2 + y^2)^{1/2}$. In this case, the cylindrical symmetry is preserved by the dynamics so that for any $t > 0$, $\psi(t, x, y, z) = \psi(t, r, z)$ and the time evolution of $\psi(t, r, z)$ is then governed by the 2D equation

$$i \frac{\partial \psi}{\partial t} = \left[\frac{\omega_x}{\omega_z} \left(-\frac{1}{2r} \frac{\partial}{\partial r} \left(r \frac{\partial}{\partial r} \right) + \frac{r^2}{2} \right) + \left(-\frac{1}{2} \frac{\partial^2}{\partial z^2} + \frac{z^2}{2} \right) + \lambda |\psi|^2 \right] \psi, \quad (15)$$

set on the spatial domain $\mathbb{R}^+ \times \mathbb{R}$. Defining a new function $\chi(t, r, z)$ on the space domain \mathbb{R}^2 by

$$\chi(t, r, z) = \begin{cases} \psi(t, r, z) & \text{if } r > 0 \\ \psi(t, -r, z) & \text{if } r < 0 \end{cases}$$

it occurs that χ satisfies

$$i \frac{\partial \chi}{\partial t} = \left[\frac{\omega_x}{\omega_z} \left(-\frac{1}{2} \frac{\partial^2}{\partial r^2} + \frac{r^2}{2} \right) + \left(-\frac{1}{2} \frac{\partial^2}{\partial z^2} + \frac{z^2}{2} \right) - \frac{\omega_x}{\omega_z} \frac{1}{2r} \frac{\partial}{\partial r} + \lambda |\chi|^2 \right] \chi \quad (16)$$

on the space domain \mathbb{R}^2 , and that, by construction, the function $r \mapsto \chi(t, r, z)$ is even. A spectral Galerkin approximation is obtained by expanding the wave function on the spectral tensor basis set

$$(\phi_{2n_r}(r) \phi_{n_z}(z))_{0 \leq n_r \leq N_r, 0 \leq n_z \leq N_z}.$$

The coefficients $(c_{n_r n_z})_{0 \leq n_r \leq N_r, 0 \leq n_z \leq N_z}$ of the expansion are solution of an equation of the same form as above,

$$i \frac{dC}{dt}(t) = hC(t) + \lambda F(C(t)).$$

The main difference is that in this case, the linear map h takes into account the operator $-\frac{1}{2r} \frac{\partial}{\partial r}$:

$$[hC]_{n_r n_z} = \left[\frac{\omega_x}{\omega_z} \left(n_r + \frac{1}{2} \right) + \left(n_z + \frac{1}{2} \right) \right] C_{n_r n_z} - \frac{1}{2} \frac{\omega_x}{\omega_z} \sum_{m_r=0}^{N_r} \left(\frac{1}{r} \frac{d\phi_{2m_r}}{dr}, \phi_{2n_r} \right)_{L^2} C_{m_r n_z}.$$

Let us remark that the scalar product $\left(\frac{1}{r} \frac{d\phi_{2m_r}}{dr}, \phi_{n_r} \right)_{L^2}$ is well defined since the first derivative of ϕ_{2n_r} is of the form $r P_{2n_r}(r) e^{-r^2/2}$ where P_{2n_r} is a polynomial of degree $2n_r$; in addition, it can be computed exactly by numerical integration with $2n_r$ Gauss points. It is worth pointing out that the ‘‘Hamiltonian’’ in (16) is not self-adjoint because of the term $-\frac{1}{2r} \frac{\partial}{\partial r}$ and that the L^2 norm of $\chi(t)$ is not a conserved quantity; on the other hand, the L^2 norm of $\chi(t)$ for the measure $r dr dz$ is conserved.

III. TIME DISCRETIZATION

When a spectral Galerkin method is used to discretize the space variables, one ends up with a finite dimensional dynamical system of the form

$$i \frac{dC}{dt}(t) = hC(t) + \lambda F(C(t)), \tag{17}$$

with initial condition $C(t = 0) = C_0$. We then use a basic fourth-order Runge-Kutta method [32] to solve Eqs. (17). Let us mention that, as the Hamiltonian character of the NLSE is preserved by the spectral Galerkin discretization, it would be possible to resort to symplectic methods [33]; such algorithms, which are particularly advised for long time evolution, are however not tested in the present work.

We will also use a grid method, based on the split-operator method, to serve as a benchmark for the spectral algorithm we have just detailed. We recall below the main features of this approach.

The wave function at time $\tau + \Delta\tau$ can be obtained from the wave function at τ according to

$$\psi(\tau + \Delta\tau) = \hat{U}(\tau, \tau + \Delta\tau)\psi(\tau), \quad (18)$$

with the propagator $\hat{U}(\tau, \tau + \Delta\tau)$ being expressed, for sufficiently small intervals $\Delta\tau$, as

$$\hat{U}(\tau, \tau + \Delta\tau) = \exp[-iH(\tau)\Delta\tau], \quad (19)$$

where $H(\tau)$ is the Hamiltonian of Eq. (4). As the potential and non-linear components of the Gross-Pitaevskii Hamiltonian do not commute with the kinetic operator, we apply the split-operator method [34] to obtain

$$\exp[-iH(\tau)\Delta\tau] = \exp\left[-iT\frac{\Delta\tau}{2}\right] \exp[-i(V + \lambda|\psi|^2)\Delta\tau] \exp\left[-iT\frac{\Delta\tau}{2}\right] + O(\Delta\tau^3), \quad (20)$$

with T the kinetic operator and V the trapping potential. The middle term is diagonal in position space, while the kinetic part is diagonal in momentum space. A Fast Fourier Transform is thus used before application of the kinetic operator, followed by the inverse transform. Note that if the intermediate wave function at time $\tau + \Delta\tau$ is not needed, the two successive kinetic operators half-steps can be combined. From a previous study [35], it appears that the split-operator method is the fastest algorithm for solving a NLSE on a grid.

IV. RESULTS

The first test we perform is the propagation of the ground stationary state (obtained from the time-independent GPE solved by a method based on the Optimal Damping Algorithm [36, 37, 38]), while monitoring the value of the coefficients $c(\tau)$ of the expansion (13). For the spherically symmetric case, we require that the relative error on the c_0 coefficient (which has the largest absolute value) be inferior to 10^{-8} , i.e., $||c_0(\tau)|^2 - |c_0(\tau = 0)|^2| / |c_0(\tau = 0)|^2 \leq 10^{-8} \forall \tau \in [0, 100]$. This criterion also results in an absolute error of all coefficients $|c_n(\tau)|^2 - |c_n(\tau = 0)|^2 \leq 10^{-8}$. We have also checked that the phase of the coefficients is correct, by calculating $|c_n(\tau) - c_n(\tau = 0)e^{-i\mu\tau}|^2 / |c_n(\tau)|^2$, where μ is the chemical potential of the ground stationary state of the GPE [6], and this value indeed is less than 10^{-12} .

In this 1D case, we need $N = 20$ basis functions for $\lambda = 100$, and the resulting time-step for the Runge-Kutta propagator is $\Delta\tau = 0.005$. If $\lambda = 1000$, the basis set used should be slightly larger, $N = 26$, with a smaller time step $\Delta\tau = 0.0025$ to insure that the above error criteria are met. The resulting propagation time up to $\tau = 100$ is 8.9 s for $\lambda = 100$ (calculated on an Athlon 1.2 GHz processor running under Linux, using the NAG Fortran 90 compiler at the -O level of optimization) and 28.3 s for $\lambda = 1000$. If we double the size of the basis set, we get a CPU time of 32.9 s for $\lambda = 100$, showing the expected $O(N^2)$ scaling of the algorithm in 1D.

Comparing now with the grid method described in Sec. III, we use $N_p = 64$ grid points in the range $-8 \leq r \leq 8$. The time step used is $\Delta\tau = 0.00025$, resulting in a propagation time of 10.3 s, which is slightly longer than what we obtain using the Runge-Kutta method.

We now apply our algorithm to study the dynamics of trapped condensates. Referring again to the spherically symmetric case, we start with the stationary ground state for an isotropic trap frequency ω . We then let this initial state ψ_0 evolve in a trap of frequency $\omega/2$, as illustrated in Fig. 1, corresponding to an experiment where the frequency of the potential trapping the condensate would be instantaneously reduced by a factor of 2. The corresponding time-evolving wave function $|\psi(t, r)|^2$ is shown in Fig. 2, for $\lambda = 10$. We must note that the values of λ we give correspond to the condensate in the initial ω -frequency trap, the effective value being used for the time evolution is thus scaled by $1/\sqrt{2}$ [see Eq. (5)], while τ is rescaled with respect to the final trap frequency $\omega/2$. We can see the “breathing” of the condensate as it expands and recontracts in the trap.

It is also interesting to look at the effect of the value of the non-linear parameter on the breathing frequency of the condensate, as seen in Fig. 3. First, we note that the initial density at the center of the trap is lower for bigger values of λ , which is expected because of the corresponding higher interparticle repulsion. Starting from an unperturbed harmonic oscillator ($\lambda = 0$), for which the complete cycle time is $\tau = 4\pi$ with recurrences every $\tau = \pi$, we observe that the oscillation frequency of the condensate in the trap increases with a greater value of λ .

For the 3D case, we will study the scissors mode [39, 40] of a trapped condensate. We consider a pancake-shaped condensate, formed in an anisotropic trap with $\omega_x = \omega_y \ll \omega_z$, see Fig. 4. The y and z axes of the trap are instantaneously rotated, at $t = 0$, by angle θ around the x axis. The condensate then starts to oscillate in the trap, leading to the

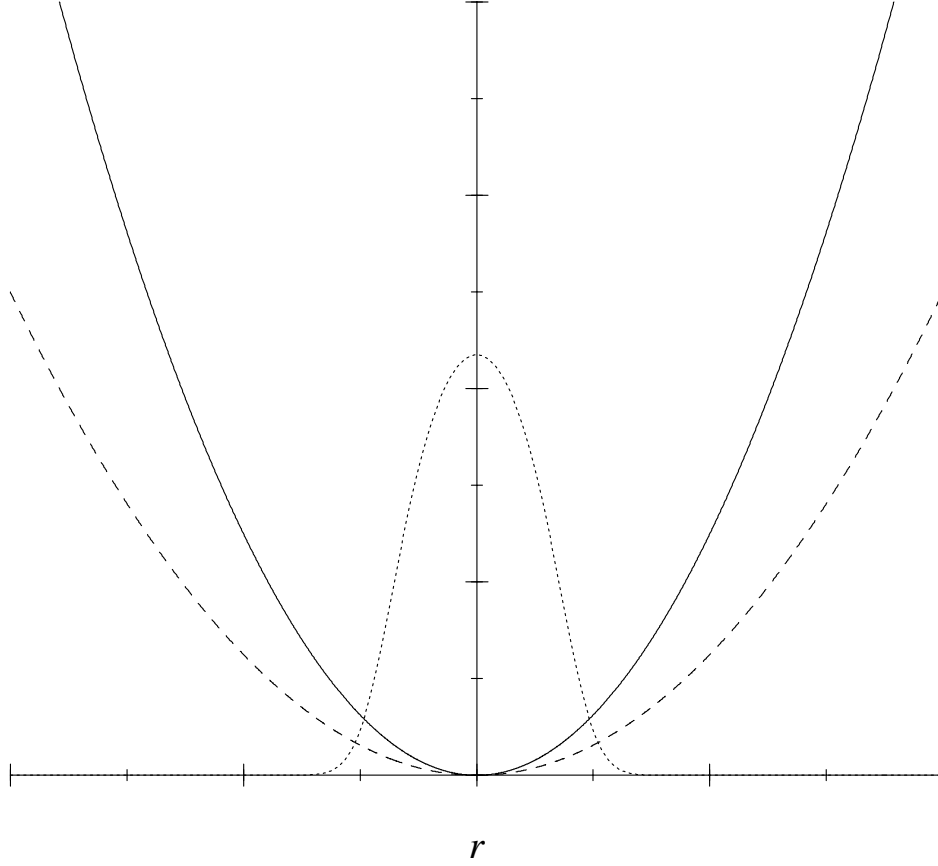


FIG. 1: Trapping potentials ω (solid line) and $\omega/2$ (dashed line) used to simulate the breathing modes of a condensate. The wave function $|\psi(r)|^2$ of the stationary state for potential ω with $\lambda = 100$ is also given (dotted line).

so-called scissors mode.

Using the parameters of the experiment of Maragò *et al.* [40], we first determine the stationary state for a condensate of $N = 10^4$ ^{87}Rb atoms in a trap with $\omega_z = 255$ Hz, $\omega_x/\omega_z = \omega_y/\omega_z = 1/\sqrt{8}$, resulting in a value $\lambda = 147.1$. The condensate is then tilted by an angle of $\theta = 3.6^\circ$, with the trapping frequency ω_z reduced by 2%, resulting in a new value of $\lambda = 148.6$. We then calculate the free evolution of this tilted condensate. We report, in Fig. 5, the angle between the condensate (as determined by the main inertia axis) and the y axis, as a function of time for the free evolution of the condensate in a trap. The oscillation frequency, in these conditions, is found to be 1.105 (in rescaled units), corresponding to 276 Hz.

This simulation was done using a basis set of $N = 29$ functions in each dimension, using a

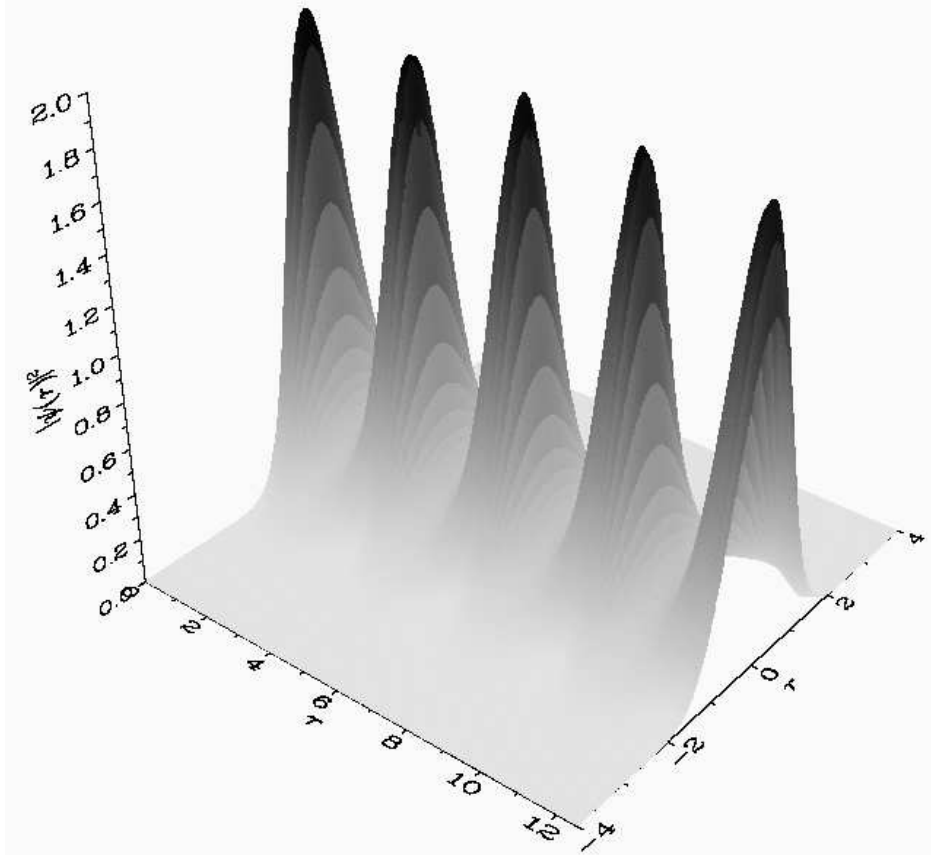


FIG. 2: “Breathing” of the condensate after expansion from a trap of frequency ω to $\omega/2$. The density profile $|\psi(r)|^2$ is given as a function of time τ (scaled with respect to the final trap frequency $\omega/2$) for an initial $\lambda = 10$ ground stationary state.

time step $\Delta\tau = 0.005$. The calculation time for a propagation of duration τ is then ≈ 1735 s. The main advantage of using a spectral Galerkin method, as noted in Sec. II B, is that in this case we can restrict the basis set in the x dimension by using only even harmonic oscillator functions, since the reflection symmetry with respect to the yOz plane is conserved. The number of functions is thus reduced to $N_x = 15$, resulting in a decrease of CPU time to ≈ 1030 s for 1 τ . This compares favorably with the grid method, for which an equivalent calculation with $64 \times 64 \times 64$ grid points takes ≈ 1700 s (using the same time step and grid spacing as for the 1D grid method).

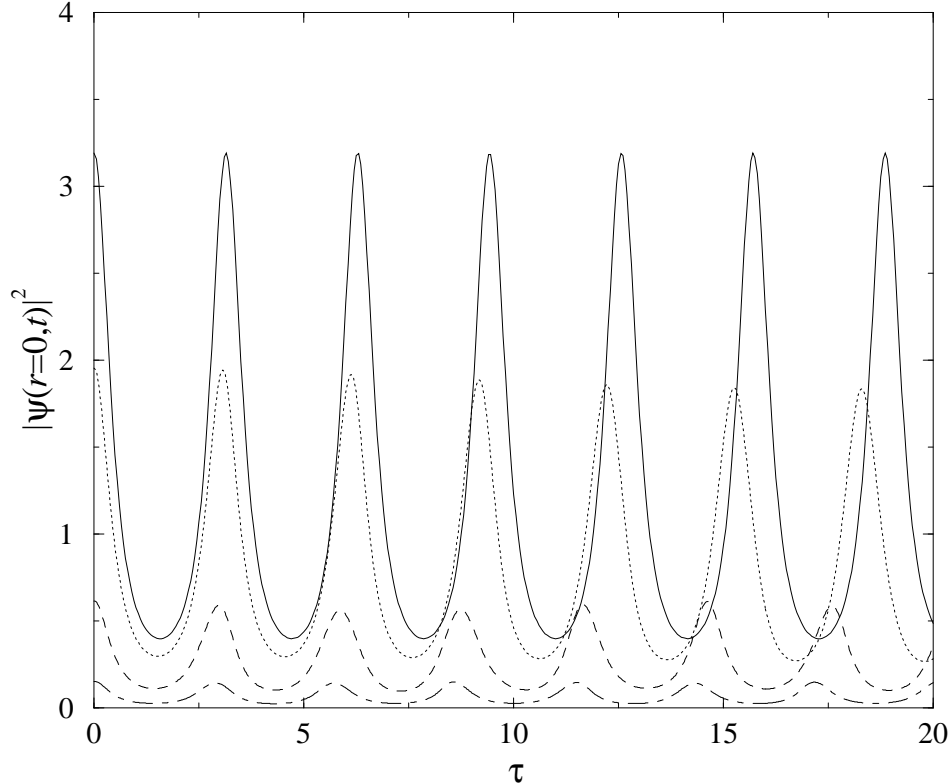


FIG. 3: “Breathing” of the condensate after expansion from a trap of frequency ω to $\omega/2$. The value of the wave function in the center of the trap, $|\psi(r=0,t)|^2$, is given as a function of time τ (scaled with respect to the final trap frequency $\omega/2$) for λ equal to 0 (solid line), 10 (dotted line), 100 (dashed line), and 1000 (dot-dashed line).

V. CONCLUSION

We have presented the application of a spectral Galerkin method to the numerical solution of the Gross-Pitaevskii equation, describing a Bose-Einstein condensate trapped in a harmonic potential well. This method is based on the decomposition of the condensate wave function on the a basis set of eigenmodes of the harmonic oscillator, while the nonlinear term in the GPE is calculated using the Gauss-Hermite quadrature. The resulting algorithm scales in $O(N^4)$ for a full 3D problem (where N is the number of basis functions used per direction), which is slightly worse than the $O(N_p^3 \log N_p)$ scaling obtained for grid-based Fourier methods. Nevertheless, the required number of basis functions needed for a given problem can be much smaller than the number of grid points N_p , allowing for fast and efficient calculations using the spectral method. We have shown how the propagation in time

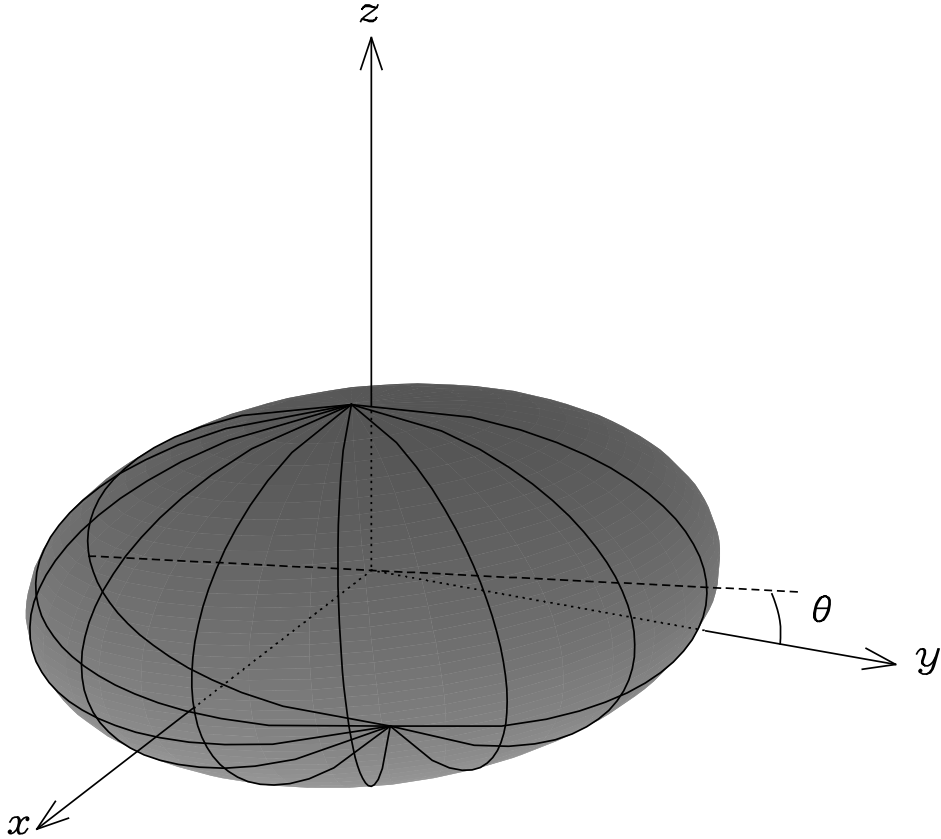


FIG. 4: Representation of the study a condensate's scissors mode. The condensate is initially tilted with respect to the trap's y and z axes by an angle θ .

can be carried out using a Runge-Kutta method on a set of coupled ordinary differential equations.

This method is akin to the DVR approach [21, 22], which relies on the fact that matrix elements of the nonlinear term can be *approximately* evaluated to sufficiently high accuracy using an N -point rule based Gauss quadratures. Our approach has the advantage that, for the basis chosen, there are no approximations in the computation of these integrals. Let us however remark that the same property can hold within the DVR method by a suitable choice of weighted polynomials. The main distinction between the usual DVR approach and our method is that we treat the kinetic and potential terms of the Hamiltonian conjointly, as detailed in Sec. II.

We have successfully applied our algorithm to simulate two different dynamical aspects of trapped BECs. Making use of the spherical symmetry of an isotropic trapping potential, we used an effective 1D equation to study the breathing of a condensate that is allowed to

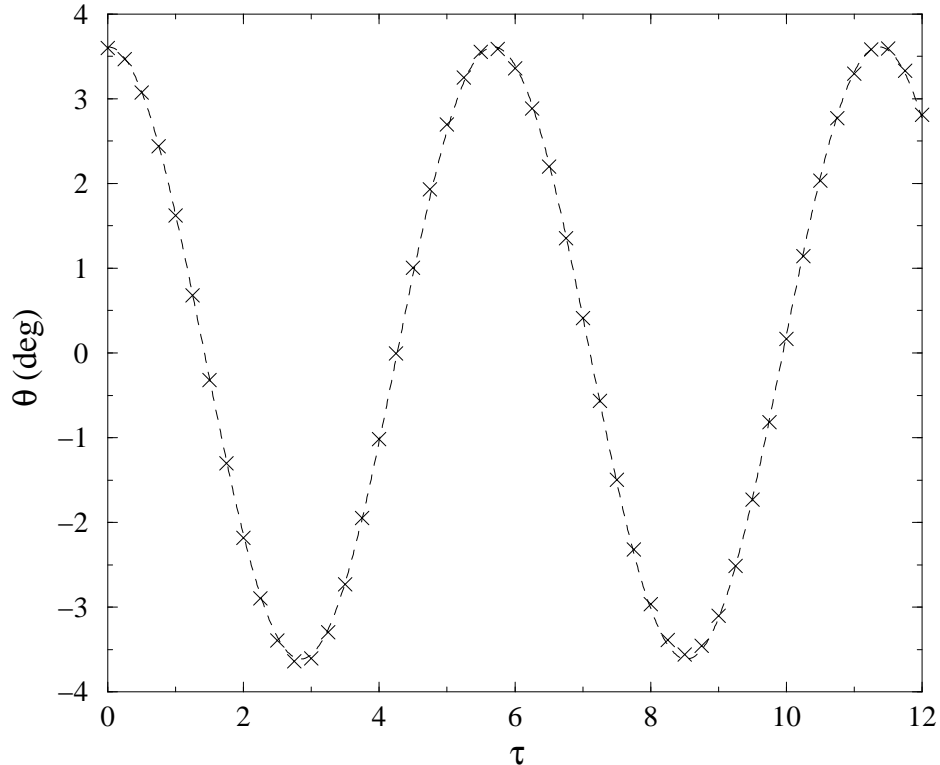


FIG. 5: Time evolution of the angle θ for the scissors mode. The crosses correspond to the angle resulting from the time-dependent calculation, along with the corresponding fit $\theta = 3.6 \cos(1.105\tau)$ (dashed line).

expand from more confining trap to a looser one. In the 3D case, we have looked at the scissors modes of a pancake-shaped condensate, for which the trapping potential is suddenly rotated along one axis.

Future work will focus on the implementation of better time-evolution algorithms on our spectral method and on its possible parallelization. Extensions will also be made to consider other terms in the Gross-Pitaevskii Hamiltonian, such as the potential created by the interaction with a laser field, or coupled Gross-Pitaevskii equations used in the simulation of two-species condensates [41] or of the formation of molecules in atomic condensates [42, 43].

Acknowledgments

We thank L. DiMenza, O. Dulieu, J. Mary, F. Masnou-Seeuws, and P. Pellegrini for stimulating discussions. Part of this work was carried out using the computer resources of IDRIS (Orsay, France).

-
- [1] M. H. Anderson, J. R. Ensher, M. R. Matthews, C. E. Wieman, and E. A. Cornell, *Science* **269**, 198 (1995).
 - [2] C. C. Bradley, C. A. Sackett, J. J. Tollett, and R. G. Hulet, *Phys. Rev. Lett.* **75**, 1687 (1995).
 - [3] K. B. Davis, M.-O. Mewes, M. R. Andrews, N. J. van Druten, D. S. Durfee, D. M. Kurn, and W. Ketterle, *Phys. Rev. Lett.* **75**, 3969 (1995).
 - [4] E. P. Gross, *Nuovo Cimento* **20**, 454 (1961).
 - [5] L. P. Pitaevskii, *Sov. Phys. JETP* **13**, 451 (1961).
 - [6] F. Dalfovo, S. Giorgini, L. P. Pitaevskii, and S. Stringari, *Rev. Mod. Phys.* **71**, 463 (1999).
 - [7] A. Röhrl, M. Naraschewski, A. Schenzle, and H. Wallis, *Phys. Rev. Lett.* **78**, 4143 (1997).
 - [8] K. Bongs, S. Burger, G. Birkl, K. Sengstock, W. Ertmer, K. Rzążewski, A. Sanpera, and M. Lewenstein, *Phys. Rev. Lett.* **83**, 3577 (1999).
 - [9] M. R. Matthews, B. P. Anderson, P. C. Haljan, D. S. Hall, M. J. Holland, J. E. Williams, C. E. Wieman, and E. A. Cornell, *Phys. Rev. Lett.* **83**, 3358 (1999).
 - [10] M. Modugno, F. Dalfovo, C. Fort, P. Maddaloni, and F. Minardi, *Phys. Rev. A* **62**, 063607 (2000).
 - [11] J.-P. Martikainen, K.-A. Suominen, L. Santos, T. Schulte, and A. Sanpera, *Phys. Rev. A* **64**, 063602 (2001).
 - [12] W. Hoston and L. You, *Phys. Rev. A* **53**, 4254 (1996).
 - [13] R. J. Ballagh, K. Burnett, and T. F. Scott, *Phys. Rev. Lett.* **78**, 1607 (1997).
 - [14] P. D. Drummond and K. V. Kheruntsyan, *Phys. Rev. A* **63**, 013605 (2000).
 - [15] P. A. Ruprecht, M. J. Holland, K. Burnett, and M. Edwards, *Phys. Rev. A* **51**, 4704 (1995).
 - [16] S. K. Adhikari, *Phys. Rev. E* **62**, 2937 (2000).
 - [17] B. Jackson, J. F. McCann, and C. S. Adams, *J. Phys. B: At., Mol. Opt. Phys.* **31**, 4489 (1998).
 - [18] R. Baer, *Phys. Rev. A* **62**, 063810 (2000).

- [19] J. J. Tollett, C. C. Bradley, C. A. Sackett, and R. G. Hulet, *Phys. Rev. A* **51**, R22 (1995).
- [20] W. Petrich, M. H. Anderson, J. R. Ensher, and E. A. Cornell, *Phys. Rev. Lett.* **74**, 3352 (1995).
- [21] B. I. Schneider and D. L. Feder, *Phys. Rev. A* **59**, 2232 (1999).
- [22] D. L. Feder, M. S. Pindzola, L. A. Collins, B. I. Schneider, and C. W. Clark, *Phys. Rev. A* **62**, 053606 (2000).
- [23] F. Pereira Dos Santos, J. Léonard, J. Wang, C. J. Barrelet, F. Perales, E. Rasel, C. S. Unnikrishnan, M. Leduc, and C. Cohen-Tannoudji, *Phys. Rev. Lett.* **86**, 3459 (2001).
- [24] J. L. Roberts, N. R. Claussen, J. P. Burke Jr., C. H. Greene, E. A. Cornell, and C. E. Wieman, *Phys. Rev. Lett.* **81**, 5109 (1998).
- [25] T. Cazenave, *An introduction to nonlinear Schrödinger equations*, no. 26 in *Textos de Métodos Matemáticos* (Instituto de Matemática – UFRJ, Rio de Janeiro, 1996), 3rd ed.
- [26] M. Edwards, R. J. Dodd, C. W. Clark, and K. Burnett, *J. Res. Natl. Inst. Stand. Technol.* **101**, 553 (1996).
- [27] M. Edwards, R. J. Dodd, C. W. Clark, P. A. Ruprecht, and K. Burnett, *Phys. Rev. A* **53**, R1950 (1996).
- [28] C. Cohen-Tannoudji, B. Diu, and F. Laloë, *Quantum Mechanics* (Wiley, New York, 1992).
- [29] A. H. Stroud and D. Secrest, *Gaussian quadrature formulas* (Prentice-Hall, Englewood Cliffs, NJ, 1966).
- [30] P. J. Davis and I. Polonsky, in *Handbook of Mathematical Functions*, edited by M. Abramowitz and I. A. Stegun (Dover, New York, 1965), chap. 25, pp. 875–924.
- [31] Y. Maday and C. Bernardi, in *Handbook of numerical analysis*, edited by P. Ciarlet and J.-L. Lions (Elsevier, Amsterdam, 2000), vol. 5, pp. 209–486.
- [32] W. H. Press, S. A. Teukolsky, W. T. Vetterling, and B. P. Flannery, *Numerical Recipes in FORTRAN* (Cambridge University Press, Cambridge, 1992), 2nd ed.
- [33] Y.-F. Tang, L. Vázquez, F. Zhang, and V. M. Pérez-García, *Comput. Math. Appl.* **32**, 73 (1996).
- [34] M. D. Feit, J. A. Fleck, Jr., and A. Steiger, *J. Comput. Phys.* **47**, 412 (1982).
- [35] T. R. Taha and M. J. Ablowitz, *J. Comput. Phys.* **55**, 203 (1984).
- [36] E. Cancès and C. Le Bris, *Int. J. Quantum Chem.* **79**, 82 (2000).
- [37] E. Cancès, in *Mathematical Models and Methods for Ab Initio Quantum Chemistry*, edited by

- M. Defranceschi and C. Le Bris (Springer, Berlin, 2000), vol. 74 of *Lecture Notes in Chemistry*, pp. 17–43.
- [38] E. Cancès and C. M. Dion (unpublished).
- [39] D. Guéry-Odelin and S. Stringari, *Phys. Rev. Lett.* **83**, 4452 (1999).
- [40] O. M. Maragò, S. A. Hopkins, J. Arlt, E. Hodby, G. Hechenblaikner, and C. J. Foot, *Phys. Rev. Lett.* **84**, 2056 (2000).
- [41] M. Trippenbach, K. Góral, K. Rzażewski, B. Malomed, and Y. B. Band, *J. Phys. B: At., Mol. Opt. Phys.* **33**, 4017 (2000).
- [42] E. Timmermans, P. Tommasini, R. Côté, M. Hussein, and A. Kerman, *Phys. Rev. Lett.* **83**, 2691 (1999).
- [43] D. J. Heinzen, R. Wynar, P. D. Drummond, and K. V. Kheruntsyan, *Phys. Rev. Lett.* **84**, 5029 (2000).